How changing the height of the Antarctic ice sheet affects global climate: A mid-Pliocene case study

Xiaofang Huang[1, 2*], Shiling Yang[1, 2, 3*], Alan Haywood[4], Julia Tindall[4], Dabang Jiang[5, 3], Yongda Wang[1, 2, 3], Minmin Sun[1, 2, 3], Shihao Zhang[1, 2, 3]

[1]Key Laboratory of Cenozoic Geology and Environment, Institute of Geology and Geophysics, Chinese Academy of Sciences, Beijing 100029, China

[2]CAS Center for Excellence in Life and Paleoenvironment, Beijing, 100044, China

[3]College of Earth and Planetary Sciences, University of Chinese Academy of Sciences, Beijing 100049, China

[4]School of Earth and Environment, University of Leeds, Leeds, LS2 9JT, UK

[5]Institute of Atmospheric Physics, Chinese Academy of Sciences, Beijing 100029, China

*Correspondence to: X. Huang, hxf@mail.iggcas.ac.cn

S. Yang, yangsl@mail.iggcas.ac.cn

Abstract: Warming-induced topographic changes of the East Antarctic Ice Sheet (EAIS) during the Pliocene warm period could have significant influence on the climate. However, how large changes in the EAIS height could theoretically affect global climate have yet to be studied. Here, the influence of possible height changes of the EAIS on climate over the East Antarctic ice sheet region versus the rest of the globe is investigated through numerical climate modeling, using the Pliocene as a test case. As expected, the investigation reveals that the reduction of ice sheet height leads to a warmer and wetter East Antarctica. However, unintuitively, both the surface air temperature and the sea surface temperature decrease over the rest of the globe. These temperature changes result from the higher air pressure over Antarctica and the corresponding lower air pressure over extra-Antarctic regions with the reduction of EAIS height. This topography effect is further confirmed by energy balance analyses. These findings could provide insights into future climate change caused by warming-induced height reduction of the Antarctic ice sheet.

Keywords: mid-Pliocene warm period; Antarctic ice sheet; height changes; sensitivity experiments

1 Introduction

The Antarctic Ice Sheet (AIS) is the largest component (by volume) of Earth's cryosphere (Gasson and Keisling, 2020). It accounts for almost 70% of the world's freshwater, representing a potential sea-level rise of 56.6 m (Shum et al., 2008). Its evolution has received considerable attention in climate research, as it determines the surface mass balance that has a major impact on both regional and global climate (DeConto et al., 2007; Bintanja et al., 2013; Goldner et al., 2014; Colleoni et al., 2018; Golledge et al., 2019; Tewari et al., 2021a). The size of the present-day AIS is known to impinge substantially on synoptic and planetary scale atmospheric flow (Parish and Bromwich, 2007; Schmittner et al., 2011; Hakuba et al., 2012; Goldner et al., 2013; Grazioli et al., 2017), and the warming-induced topographic changes of the AIS in turn

have significant influence on the climate (Orr et al., 2008; Tewari et al., 2021a, b). However, the effect of the AIS height changes on future predictions of climate is still uncertain. One method of investigating this effect in a warmer-than-modern climate is to look back at past warm periods of Earth history, for example the Pliocene.

The mid-Pliocene warm period (~3.3–3.0 Ma) is the most recent period of relatively warm and stable climate in Earth's history, during which atmospheric CO_2 concentrations were approximately 400 ppmv (Pagani et al., 2010; Lunt et al., 2012a; Yang et al., 2018; De La Vega et al., 2020; Huang et al., 2021) and models suggested that global mean annual temperature was 1.7–5.2 °C warmer than today (Haywood et al., 2020). This period is similar to today in terms of the continent–ocean configuration and atmospheric CO_2 concentrations (Haywood et al., 2016) and has often been proposed as a climatic analog for the end of this century (Burke et al., 2018). The present atmospheric CO_2 concentration is over 410 ppmv and has reached the Pliocene level. However, due to the large thermal inertia of the oceans (Levitus et al., 2000; Back et al., 2013), the atmosphere-ocean system is still in a nonequilibrium state and the global mean temperature is projected to rise to the level of the Pliocene as early as the 2040s (Zhang, 2012; Ding et al., 2014; Jiang et al., 2016; Burke et al., 2018; Tierney et al., 2020). In this scenario, about 30% of the Antarctic mass loss amounts would occur in coming centuries (Grant et al., 2019). Therefore, we use climate model simulations of the Pliocene to investigate how large, hypothetical changes in East AIS (EAIS) height would affect the climate.

Numerical experiments have emerged as an efficient means of understanding past climates on regional and global scales (Huang et al., 2019). Based on simulations, the dynamic behavior of the AIS and its stability to the climate change have been analyzed (Raymo et al., 2006; Naish et al., 2009; Cook et al., 2013; Patterson et al., 2014; Austermann et al., 2015; Boer et al., 2015; Yamane et al., 2015; Scherer et al., 2016; Dolan et al., 2018). Here we design sensitivity experiments using a coupled climate model to investigate how perturbations in the EAIS heigh would interact with the atmospheric flow and influence the temperature and precipitation dynamics over the

East Antarctic ice sheet region and the rest of the globe.

2 Methods

2.1 Model description

The Hadley Centre coupled climate model version 3 (hereafter referred to as HadCM3) was used for this study. This model has been used extensively for studies of the Pliocene within the Pliocene Model Intercomparison Project experiments (Haywood et al., 2010, 2011; Bragg et al., 2012; Hunter et al., 2019). HadCM3 consists of two main components: an atmospheric component (HadAM3) and an oceanic component (HadOM3) (Gordon et al., 2000; Pope et al., 2000; Valdes et al., 2017). The horizontal resolution of the atmosphere model is 2.5° in latitude by 3.75° in longitude and consists of 19 layers in the vertical. The atmospheric model has a time step of 30 min and includes a radiation scheme that can represent the effects of major and minor trace gases (Edwards and Slingo, 1996). The HadOM3 spatial resolution of the ocean is 1.25° latitude by 1.25° longitude, with 20 vertical layers. The ocean model is a 'rigid lid' model, which has a time step of one hour and incorporates a thermodynamic-dynamic sea ice model with primitive (ocean drift) dynamics. The HadCM3 has been shown to well represent the broad-scale features of the Antarctic and Arctic atmospheric and oceanic circulation (Turner et al., 2006; Chapman and Walsh, 2007). The fact that the HadCM3 consistently performs well in tests against other coupled atmosphere–ocean models (Lambert and Boer, 2001; Hegerl et al., 2007; Dolan et al., 2011) increases our confidence in its palaeoclimate simulations.

2.2 Pliocene boundary conditions and experimental designs

For this study the required mid-Pliocene boundary conditions were supplied by the U.S. Geological Survey Pliocene Research Interpretations and Synoptic Mapping Group's (PRISM) dataset, specifically the latest iteration of the reconstruction known as PRISM4 (Dowsett et al., 2016). They include topography and bathymetry, coastlines, land surface properties (i.e., vegetation, soil type, and ice sheet coverage) and

atmospheric composition with respect to pre-industrial conditions. The Greenland Ice Sheet and the West Antarctic Ice Sheet, which currently store ~13 m sea-level equivalent ice (Dolan et al., 2011; Yamane et al., 2015), are thought to have largely melted during the mid-Pliocene warm period (Lunt et al., 2008; Naish et al., 2009). Therefore, our experiments focus on changing the East Antarctic Ice Sheet height (Figure 1) against its reconstructed Pliocene value. It should be noted that the surface type is still 'snow' and so there will still be high albedo in this region.

Our control simulation is started from the end of the HadCM3 contribution to PlioMIP2 simulation (Hunter et al., 2019). There is a difference between our control simulation and the PlioMIP2 simulation, namely we use dynamic vegetation while Hunter et al. (2019) uses fixed vegetation from PRISM4. we manipulate the height of the ice sheet for each sensitivity simulation on the basis of the control experiment. To evaluate the regional and global climate sensitivity to the EAIS height changes, five Pliocene modelling experiments are presented in this paper, which were identical except for the height of the EAIS: one mid-Pliocene control run (hereafter MPControl) and four sensitivity simulations with height reduced by 100% (hereafter -100%EAIS), 75% (hereafter -75%EAIS), 50% (hereafter -50%EAIS), and 25% (hereafter -25%EAIS) of the Pliocene height. All these sensitivity experiments are hypothetical scenarios and are not intended to correspond to projected future scenarios. Instead, they are designed to isolate how changes in the elevation of the EAIS would affect a warmer world.

To provide a more realistic -100%EAIS experiment, we further perform an experiment in which the EAIS is still at -100% but the land topography (away from Antarctica) is reduced by 60 m (hereafter -100%EAIS & -60-m land), to artificially raise the sea level. Locations where the land was below 60 m are set to 0 m to maintain the mid-Pliocene land sea mask, which means that there are no ocean gateway changes that could affect ocean dynamics.

The mid-Pliocene control experiment uses the East Antarctic ice sheet configuration (and all other boundary conditions) specified in the USGS PRISM4 data set. The EAIS volume is smaller during the mid-Pliocene than at the present -day, and

the reduced EAIS is equivalent of 15 m sea-level rise (Dowsett et al., 2010). All experiments (including the ice sheet sensitivity experiments) are started from the end of the HadCM3 PlioMIP2 simulation and are continued for another 500 model years allowing the modelled climate to be equilibrated to the boundary conditions. Climate statistics are based on time averages of the final 30 years for each run. The results are presented as anomalies from the control for the sensitivity experiments.

3 Results

3.1 Surface air temperature changes

Reducing the height of the EAIS experiments results in a dramatic annual mean warming over East Antarctica relative to the MPControl experiment (Figure 2). Compared with the MPControl experiment, the East Antarctic annual mean surface temperature increases by about 5 ℃, 10 ℃, 15 ℃, and 18 ℃ with the height reduction of 25%, 50%, 75%, and 100%, respectively (Figure 2). Based on Figure 1a, the average height of the EAIS is ~3.2 kilometers, which means that every 25% reduction of the height is ~0.8 kilometer. Clearly, this surface warming occurs at a rate of ~6 ℃ per kilometer of EAIS height lost, which is confirmed by the change in temperature due to changing surface height (Figure S1) and is accompanied by a prominent surface cooling over western Antarctica and the Southern Ocean.

Contrary to Antarctic warming, reducing the height of the EAIS experiments leads to annual mean surface cooling over the rest of the globe (Figure 3). The inclusion of the -100%EAIS set of boundary conditions results in a ~1–2 ℃ mean cooling over the rest of the globe (Figure 3a). In low and equatorial regions, temperatures decrease by a minimum of 0.5–1 ℃ and cooling is at its greatest (~3 ℃) over Southern Ocean. For -75%EAIS and -50%EAIS experiments (Figures 3b, c), annual mean values for surface air temperature decrease by ~0.5 ℃ and ~1 ℃, respectively. Compared with the MPControl experiment, the surface air temperature in -25%EAIS experiment changes little (the mean value near zero; Figure 3d).

3.2 Precipitation changes

The numerical simulations show that with the height reduction of the EAIS, the annual precipitation has increased over East Antarctica and decreased over the rest of the southern hemisphere (Figure 4). Precipitation enhancements are greatest in -100%EAIS (~0.4 mm day^{-1}; Figure 4a) and smallest in -25%EAIS (~0.1 mm day^{-1}; Figure 4d). Based on Figure 4e, the annual mean precipitation of the MPControl experiment over the EAIS is ~0.4 mm day^{-1}, which means that the precipitation increases ~25% with every 25% reduction of the height. Clearly, this precipitation enhancement over East Antarctica occurs at a rate of approximately 5% per degree Celsius of temperature, which is accompanied by a precipitation deficit over the western Antarctica and the Southern Ocean. With respect to the MPControl experiment, precipitation reduces significantly over the western Antarctica and the Southern Ocean (~0.3–0.8 mm day^{-1}; Figure 4a) in the -100%EAIS experiments, but decreases slightly over those areas (~0.1–0.2 mm day^{-1}; Figure 4d) in the -25%EAIS experiments.

Annual precipitation decreases consistently over most areas on the globe in all the sensitivity experiments compared to the MPControl experiments (Figure 5). This is consistent with the decreased air temperatures (Figure 3), which reduce moisture carrying capacity of the air and lead to less precipitation. The experiment showing the greatest sensitivity in terms of precipitation response is -100%EAIS, with the anomaly varying from -2 to 0.8 mm day^{-1} (Figure 5a), while the least is -25%EAIS with a narrow anomalous range of -0.4–0.4 mm day^{-1} (Figure 5d). The spatial patterns (Figures 5a-d) show that the enhanced precipitation focuses over parts of the tropics and the 45th parallel south, while the deficit focuses over northern high latitudes and the Antarctic periphery. The largest precipitation anomaly is found in the tropics that are dominated by the intertropical convergence zone (ITCZ). In general, for most areas except the Southern Ocean, the simulations that display the largest SAT sensitivity to the prescription of EAIS height changes also exhibit the largest precipitation anomaly.

4 Discussion

4.1 Cause of the precipitation changes over Antarctica

Earlier studies have shown a clear relationship between the atmospheric circulation and precipitation dynamics, arguing that precipitation over polar regions is mostly due to orographic effects acting upon the circulation pattern passing over the region (Schmittner et al., 2011; Hakuba et al., 2012; Goldner et al., 2013; Tewari et al., 2021a). The mechanical obstruction by the ice sheet prevents the moisture laden winds from penetrating inland (Parish and Bromwich, 2007; Grazioli et al., 2017; Tewari et al., 2021b). The gravity-driven katabatic flow, which carries dense cold air mass out from the polar plateau, impedes a poleward shift of the moisture laden winds (Goldner et al., 2013; Tewari et al., 2021b). Therefore, the weakened katabatic flow, due to the successive topographic reduction, leads to an elevated moisture transport into the continent (Figure 7), thereby increasing precipitation over EAIS (Figure 4).

Figure 6 shows the magnitude and direction of the low-level wind at 850 hPa over the Southern Hemisphere and the corresponding changes observed in their strength due to orographic perturbations in individual simulations. In the MPControl experiment, strong surface westerly winds encircle the East Antarctic continent, extending from ~60°S to the continental periphery (Figure 6a), indicating the blocking effect of the EAIS (Tewari et al., 2021b).

Upon successive reduction of the EAIS height (Figures 6b–e), the westerly flow becomes weaker between 60°S and 90°S and penetrates gradually into the eastern continent. The EAIS height reductions of 100% and 75% cause a poleward shift in the surface flows (Figures 6b, c), which even circulates around the Southern Pole. In contrast, reductions by 50% and 25% cause little change in the surface winds. In this context, sustained attention needs to be paid to changes in the height of AIS in future warming and their effect on atmospheric circulation and precipitation dynamics over the region.

To further investigate the mechanism for the precipitation changes over Antarctica, we analyzed the annual water vapor flux over this region. The results show that in the MPControl experiment, strong westerly flow encircle the East Antarctic continent,

extending from ~60°S to the continental periphery (Figure 7a). In contrast, with the height reduction of the EAIS, the anomalies show easterly flow encircle the East Antarctic continent, extending from ~60°S to the continental periphery (Figures 7b-e). These mean that the water vapor flux decrease over the region from ~60°S to the continental periphery, which is consistent with the decreased precipitation over this region (Figure 4). Over the East Antarctica, upon successive reduction of the EAIS height, the westerly flow penetrates gradually into the eastern continent and bring more and more water vapor into this region (Figures 7b-e), which is consistent with the increased precipitation over the eastern continent (Figure 4).

4.2 Causes of global temperature changes

In order to identify factors controlling the air temperature changes with the height reduction of the EAIS, energy balance analyses (Heinemann et al., 2009; Lunt et al., 2012b; Hill et al., 2014) between the sensitivity experiments and MPControl experiment have been completed. This approach has been used in palaeoclimate simulations to understand the simulated temperature changes (Donnadieu et al., 2006; Murakami et al., 2008; Hill et al., 2014; Lunt et al., 2021; Baatsen et al., 2022), and more details about how to conduct this energy balance analysis can be found in Hill et al. (2014). The results show that the heat transport from the rest of the globe, especially from the proximal Southern Ocean, to Antarctica is the primary factor influencing the temperature changes over Antarctica and its contribution rate reaches ~52% (Figure 8). However, over the rest of the globe, the heat transport is the secondary factor influencing the temperature decreasing (Figure 3) and except the -25%EAIS experiment, the contribution in other sensitivity experiments reaches ~25% (Figure 8).

The secondary factor controlling the Antarctic temperature is ‘Topography+GHG’ and its contribution rate reaches ~30% (Figure 8). In contrast, over the rest of the globe, ‘Topography+GHG’ is the primary factor influence the temperature changes and the contribution is ~48%. All experiments were forced with the same trace gases, therefore the ‘Topography+GHG’ factor represents both the direct effect of ice sheet height

changes on temperature and some indirect effects via GHG feedbacks.

The direct effect of ice sheet height changes on temperature can be explained by the surface air pressure changes. As shown in Figure 9, the surface air pressure increases over Antarctica and decreases over elsewhere, which is similar to the spatial pattern of the air temperature changes (Figure 3). With the reduction of the EAIS height, the air mass increases over Antarctica, which at the expense of that over the rest of the globe, leading to higher air pressure over Antarctica and lower air pressure over extra-Antarctic regions (Figure 9). According to the ideal gas law (Clapeyron, 1834), lower air pressures correspond with lower air temperatures, which may explain the temperature contrast between Antarctica and extra-Antarctic regions.

The possible indirect effect includes that 1) when the EAIS is reduced, the atmosphere will become thicker in this region, which will lead to more greenhouse gases in the column and hence more warming; 2) the warmer atmosphere will be able to hold more water vapor. Our results are useful for better understanding the effect of the AIS height changes on climate.

4.3 Modelling methodological limitations

In the present study, the HadCM3 model was used to investigate the influence of the height reduction of the EAIS on temperature, precipitation, atmospheric circulation, surface air pressure, and the energy transport at the regional and global scales. The objective of these simulations was to quantify how the existence of the EAIS would affect the mid-Pliocene climate. It can be concluded from the present findings that reduction in the EAIS height during the mid-Pliocene warm period induces warming and wetting over the East Antarctica, and the cooling over the extra-Antarctica regions. The Antarctic surface warming and coastal cooling due to the height reduction of Antarctic ice sheet were also observed in the modern Antarctic height reduction sensitivity experiments using the CAM5.1 model (Tewari et al., 2021a). It should be noted that the effect of changes in the surface albedo, sea level, and continental margins, which would undoubtedly occur with such orographic variations, have not been explicitly taken into account in the present idealized simulations. Despite these caveats,

we expect that the dynamical influence of the EAIS over the Antarctic presented herein will persist even in their presence.

Another modelling limitation is that the water contained in Antarctica did not get redistributed over the ocean when we reduced the EAIS height. This is because the HadCM3 is a 'rigid lid' model, which means the sea-level is essentially fixed. The "-100%EAIS & -60-m land" experiment enables us to assess how pressure changes due to the loss of the EAIS will affect the global temperature (Figure 10). The changes between this experiment and the MPControl experiment show that the surface air temperature and surface air pressure (Figure 10) both show a similar spatial pattern with the changes between the -100%EAIS and MPControl experiments. However, the results also show that 1) the pressure difference over the land (Figure 10a) is much smaller than that in Figure 9a, but there is still a pressure difference over the ocean; and 2) the temperature over the land away from Antarctica is still colder (Figure 10b), although is not by as much in Figure 3a. Clearly, the cooling away from Antarctica is robust, and would occur even if sea level changes were accounted for. Therefore, global temperature changes are likely to result from changes in the height of the EAIS.

5 Conclusions

The sensitivity of climate to the height changes of East Antarctic ice sheet during the mid-Pliocene warm period has been conducted using the HadCM3 model. The results show that, due to a successive topographic reduction in the East Antarctic ice sheet, i) the surface air temperature over EAIS increases at a rate of approximately 6 ℃ per kilometer of EAIS height lost; ii) the precipitation over EAIS increases at a rate of approximately 5% per degree Celsius of temperature; iii) the surface air temperature and the sea surface temperature both decrease over the rest of the globe; and iv) the surface air pressure increases over the East Antarctica, while decreasing elsewhere. Energy balance analyses show that the heat transport, which results from the topography changes of Antarctica, is mainly responsible for the temperature changes.

Data availability

The data presented in the Figures can be downloaded from the server located at the School of Earth and Environment of the University of Leeds. Contact Julia Tindall (j.c.tindall@leeds.ac.uk) for access.

Author contributions

Xiaofang Huang contributes to the experiments, data analysis, idea and draft paper. Shiling Yang provides the funding acquisition, and helps to revise the draft. Alan Haywood contributes to the experiments design and helps to revise the draft. Julia Tindall assists to perform the experiments and helps to revise the draft. Dabang Jiang helps to revise the draft. All authors make contributions to the paper discussion.

Competing interests

The authors declare that they have no conflict of interest

Acknowledgements

This study was supported by the National Natural Science Foundation of China (41725010 and 42107472), the Strategic Priority Research Program of the Chinese Academy of Sciences (XDB26000000 and XDB31000000) and the Key Research Program of the Institute of Geology & Geophysics, CAS (IGGCAS-201905). The authors thank Steven Phipps and two anonymous reviewers for critical comments.

References

Austermann, J., Pollard, D., Mitrovica, J. X., Moucha, R., Forte, A. M., DeConto, R. M., Rowley, D.B., and Raymo, M. E.: The impact of dynamic topography change on Antarctic ice sheet stability during the mid-Pliocene warm period, Geology, 43(10), 927–930, doi:10.1130/G36988.1, 2015.

Baatsen, M. L., von der Heydt, A. S., Kliphuis, M. A., Oldeman, A. M., and Weiffenbach, J. E.: Warm mid-Pliocene conditions without high climate sensitivity:

the CCSM4-Utrecht (CESM 1.0.5) contribution to the PlioMIP2, Clim. Past, 18(4), 657–679, 2022.

Back, L., Russ, K., Liu, Z., Inoue, K., Zhang, J., and Otto-Bliesner, B.: Global hydrological cycle response to rapid and slow global warming, J. Clim., 26(22), 8781–8786, doi:10.1175/jcli-d-13-00118.1, 2013.

Bintanja, R., van Oldenborgh, G. J., Drijfhout, S. S., Wouters, B., and Katsman, C. A.: Important role for ocean warming and increased ice-shelf melt in Antarctic sea-ice expansion, Nat. Geosci., 6(5), 376–379, doi:10.1038/ngeo1767, 2013.

Boer, B. D., Dolan, A. M., Bernales, J., Gasson, E., Goelzer, H., Golledge, N. R., Sutter, J., Huybrechts, P., Lohmann, G., Rogozhina, I., Abe-Ouchi, A., Saito, F., and Van De Wal, R. S.: Simulating the Antarctic ice sheet in the late-Pliocene warm period: PLISMIP-ANT, an ice-sheet model intercomparison project, Cryosphere, 9(3), 881–903, doi:10.5194/tc-9-881-2015, 2015.

Bragg, F. J., Lunt, D. J., and Haywood, A. M.: Mid-Pliocene climate modelled using the UK Hadley Centre Model: PlioMIP Experiments 1 and 2, Geosci. Model Dev., 5, 1109–1125, doi:10.5194/gmd-5-1109-2012, 2012.

Burke, K. D., Williams, J. W., Chandler, M. A., Haywood, A. M., Lunt, D. J., and Otto-Bliesner, B. L.: Pliocene and Eocene provide best analogs for near-future climates, Proc. Natl. Acad. Sci. USA, 115(52), 13288–13293, doi:10.1073/pnas.1809600115, 2018.

Chapman, W. L., and Walsh, J. E.: Simulations of Arctic temperature and pressure by global coupled models, J. Clim., 20(4), 609–632, doi:10.1175/jcli4026.1, 2007.

Clapeyron, É.: Mémoire sur la puissance motrice de la chaleur. Journal de l'École polytechnique, 14, 153–190, 1834.

Colleoni, F., De Santis, L., Siddoway, C. S., Bergamasco, A., Golledge, N. R., Lohmann, G., Passchier, S., and Siegert, M. J.: Spatio-temporal variability of processes across Antarctic ice-bed–ocean interfaces, Nat. Commun., 9(1), 1–14, doi:10.1038/s41467-018-04583-0, 2018.

Cook, C. P., Van De Flierdt, T., Williams, T., Hemming, S. R., Iwai, M., Kobayashi, M.,

Jimenez-Espejo, F. J., Escutia, C., González, J. J., Khim, McKay, B., R. M., Passchier, S., Bohaty, S. M., Riesselman, C. R., Tauxe, L., Sugisaki, S., Galindo, A. L., Patterson, M. O., Sangiorgi, F., Pierce, E. L., Brinkhuis, H., Klaus, A., Fehr, A., Bendle, J. A. P., Bijl, P. K., Carr, S. A., Dunbar, R. B., Flores, J. A., Hayden, T. G., Katsuki, K., Kong, G. S., Nakai, M., Olney, M. P., Pekar, S. F., Pross, J., Röhl, U., Sakai, T., Shrivastava, P. K., Stickley, C. E., Tuo, S., Welsh, K., and Yamane, M.: Dynamic behaviour of the East Antarctic ice sheet during Pliocene warmth, Nat. Geosci., 6(9), 765–769, doi:10.1038/NGEO1889, 2013.

DeConto, R., Pollard, D., and Harwood, D.: Sea ice feedback and Cenozoic evolution of Antarctic climate and ice sheets, Paleoceanography, 22(3), PA3214, doi:10.1029/2006pa001350, 2007.

De La Vega, E., Chalk, T. B., Wilson, P. A., Bysani, R. P., and Foster, G. L.: Atmospheric CO_2 during the mid-Piacenzian warm period and the M2 glaciation, Sci. Rep., 10(1), 1–8, doi:10.1038/s41598-020-67154-8, 2020.

Ding, Y., Si, D., Sun, Y., Liu, Y., and Song, Y.: Inter-decadal variations, causes and future projection of the Asian summer monsoon, Eng. Sci., 12(2), 22–28, doi:10.1002/joc.1759, 2014.

Dolan, A. M., De Boer, B., Bernales, J., Hill, D. J., and Haywood, A. M.: High climate model dependency of Pliocene Antarctic ice-sheet predictions, Nat. Commun., 9(1), 1–12, doi:10.1038/s41467-018-05179-4, 2018.

Dolan, A. M., Haywood, A. M., Hill, D. J., Dowsett, H. J., Hunter, S. J., Lunt, D. J., and Pickering, S. J.: Sensitivity of Pliocene ice sheets to orbital forcing, Palaeogeogr. Palaeoecl., 309, 98–110, doi:10.1016/j.palaeo.2011.03.030, 2011.

Donnadieu, Y., Pierrehumbert, R., Jacob, R., and Fluteau, F.: Modelling the primary control of paleogeography on Cretaceous climate, Earth Planet. Sc. Lett., 248, 426–437, doi: 10.1016/j.epsl.2006.06.007, 2006.

Dowsett, H., Dolan, A., Rowley, D., Moucha, R., Forte, A. M., Mitrovica, J. X., Pound, M., Salzmann, U., Robinson, M., Chandler, M., Foley, K., and Haywood, A.: The PRISM4 (mid-Piacenzian) paleoenvironmental reconstruction, Clim. Past, 12,

1519–1538, doi:10.5194/cp-12-1519-2016, 2016.

Dowsett, H. J., Robinson, M., Haywood, A. M., Salzmann, U., Hill, D., Sohl, L. E., Chandler, M., Williams, M., Foley, K., Stoll, D. K.: The PRISM3D paleoenvironmental reconstruction. Stratigraphy, 7, 123–139, doi:10.1111/j.1475-4983.2010.00949.x, 2010.

Edwards, J. M., and Slingo, A.: Studies with a flexible new radiation code. I: Choosing a configuration for a large-scale model, Q. J. R. Meteorol. Soc., 122(531), 689–719, doi:10.1002/qj.49712253107, 1996.

Gasson, E. G., and Keisling, B. A.: The Antarctic Ice Sheet, Oceanography, 33(2), 90–100, doi:10.5670/oceanog.2020.208, 2020.

Goldner, A., Herold, N., and Huber, M.: Antarctic glaciation caused ocean circulation changes at the Eocene–Oligocene transition, Nature, 511(7511), 574–577, 2014.

Goldner, A., Huber, M., and Caballero, R.: Does Antarctic glaciation cool the world? Clim. Past, 9(1), 173–189, doi:10.5194/cp-9-173-2013, 2013.

Golledge, N. R., Keller, E. D., Gomez, N., Naughten, K. A., Bernales, J., Trusel, L. D., and Edwards, T. L.: Global environmental consequences of twenty-first-century ice-sheet melt, Nature, 566(7742), 65–72, doi:10.1038/s41586-019-0889-9, 2019.

Gordon, C., Cooper, C., Senior, C. A., Banks, H., Gregory, J. M., Johns, T. C., Mitchell, J. F. B., and Wood, R. A.: The simulation of SST, sea ice extents and ocean heat transports in a version of the Hadley Centre coupled model without flux adjustments, Clim. Dynam., 16(2), 147–168, doi:10.1007/s003820050010, 2000.

Grant, G. R., Naish, T. R., Dunbar, G. B., Stocchi, P., Kominz, M. A., Kamp, P. J., Tapia, C. A., McKay, R. M., Levy, R. H., Patterson, M. O.: The amplitude and origin of sea-level variability during the Pliocene epoch, Nature, 574(7777), 237–241, doi:10.1038/s41586-019-1619-z, 2019.

Grazioli, J., Madeleine, J. B., Gallée, H., Forbes, R. M., Genthon, C., Krinner, G., and Berne, A.: Katabatic winds diminish precipitation contribution to the Antarctic ice mass balance, Proc. Natl. Acad. Sci. USA, 114(41), 10858–10863, doi:10.1073/pnas.1707633114, 2017.

Hakuba, M. Z., Folini, D., Wild, M., and Schär, C.: Impact of Greenland's topographic height on precipitation and snow accumulation in idealized simulations, J. Geophys. Res.: Atmos., 117, D09107, doi:10.1029/2011JD017052, 2012.

Haywood, A. M., Dowsett, H. J., and Dolan, A. M.: Integrating geological archives and climate models for the mid-Pliocene warm period, Nat. Commun., 7(1), 1–14, doi:10.1038/ncomms10646, 2016.

Haywood, A. M., Dowsett, H. J., Otto-Bliesner, B., Chandler, M. A., Dolan, A. M., Hill, D. J., Lunt, D. J., Robinson, M. M., Rosenbloom, N., Salzmann, U., and Sohl, L. E.: Pliocene Model Intercomparison Project (PlioMIP): experimental design and boundary conditions (Experiment 1), Geosci. Model Dev., 3, 227–242, doi:10.5194/gmd-3-227-2010, 2010.

Haywood, A. M., Dowsett, H. J., Robinson, M. M., Stoll, D. K., Dolan, A. M., Lunt, D. J., Otto-Bliesner, B., and Chandler, M. A.: Pliocene Model Intercomparison Project (PlioMIP): experimental design and boundary conditions (Experiment 2), Geosci. Model Dev., 4, 571–577, doi:10.5194/gmd-4-571-2011, 2011.

Haywood, A. M., Tindall, J. C., Dowsett, H. J., Dolan, A. M., Foley, K. M., Hunter, S. J., Hill, D. J., Chan, W.-L., Abe-Ouchi, A., Stepanek, C., Lohmann, G., Chandan, D., Peltier, W. R., Tan, N., Contoux, C., Ramstein, G., Li, X., Zhang, Z., Guo, C., Nisancioglu, K. H., Zhang, Q., Li, Q., Kamae, Y., Chandler, M. A., Sohl, L. E., Otto-Bliesner, B. L., Feng, R., Brady, E. C., von der Heydt, A. S., Baatsen, M. L. J., and Lunt, D. J.: The Pliocene Model Intercomparison Project Phase 2: large-scale climate features and climate sensitivity, Clim. Past, 16, 2095–2123, https://doi.org/10.5194/cp-16-2095-2020, 2020.

Hegerl, G. C., Zwiers, F. W., Braconnot, P., Gillett, N. P., Luo, Y., Marengo Orsini, J. A., Nicholls, N., Penner, J. E., and Stott. P. A.: Understanding and attributing climate change, Solomon, S., Qin, D., Manning, M., Chen, Z., Marquis, M., Averyt, K. B., Tignor, M., Miller, H. L. (Eds.), Climate Change 2007: The Physical Science Basis, Contribution of Working Group I to the Fourth Assessment Report of the Intergovernmental Panel on Climate Change, Cambridge University Press,

Cambridge, United Kingdom, 2007.

Heinemann, M., Jungclaus, J. H., and Marotzke, J.: Warm Paleocene/Eocene climate as simulated in ECHAM5/MPI-OM, Clim. Past, 5, 785–802, doi:10.5194/cp-5-785-2009, 2009.

Hill, D. J., Haywood, A. M., Lunt, D. J., Hunter, S. J., Bragg, F. J., Contoux, C., Stepanek, C., Sohl, L., Rosenbloom, N. A., Chan, W.-L., Kamae, Y., Zhang, Z., Abe-Ouchi, A., Chandler, M. A., Jost, A., Lohmann, G., Otto-Bliesner, B. L., Ramstein, G., and Ueda, H.: Evaluating the dominant components of warming in Pliocene climate simulations, Clim. Past, 10(1), 79–90, doi:10.5194/cp-10-79-2014, 2014.

Huang, X., Jiang, D., Dong, X., Yang, S., Su, B., Li, X., Tang Z., and Wang, Y.: Northwestward migration of the northern edge of the East Asian summer monsoon during the mid-Pliocene warm period: Simulations and reconstructions, J. Geophys. Res.: Atmos., 124(3), 1392–1404, doi:10.1029/2018JD028995, 2019.

Huang, X., Yang, S., Haywood, A., Jiang, D., Wang, Y., Sun, M., Tang, Z., and Ding, Z.: Warming-Induced Northwestward Migration of the Asian Summer Monsoon in the Geological Past: Evidence from Climate Simulations and Geological Reconstructions, J. Geophys. Res.: Atmos., 126(18), e2021JD035190, doi:10.1029/2021JD035190, 2021.

Hunter, S. J., Haywood, A. M., Dolan, A. M., and Tindall, J. C.: The HadCM3 contribution to PlioMIP phase 2, Clim. Past, 15(5), 1691–1713, doi:10.5194/cp-15-1691-2019, 2019.

Lambert, S. J., and Boer, G. J.: CMIP1 evaluation and intercomparison of coupled climate models, Clim. Dynam., 17(2), 83–106, doi:10.1007/pl00013736, 2001.

Levitus, S., Antonov, J. I., Boyer, T. P., and Stephens, C.: Warming of the world ocean, Science, 287(5461), 2225–2229, doi:10.1126/science.287.5461.2225, 2000.

Lunt, D. J., Bragg, F., Chan, W.-L., Hutchinson, D. K., Ladant, J.-B., Morozova, P., Niezgodzki, I., Steinig, S., Zhang, Z., Zhu, J., Abe-Ouchi, A., Anagnostou, E., de

Boer, A. M., Coxall, H. K., Donnadieu, Y., Foster, G., Inglis, G. N., Knorr, G., Langebroek, P. M., Lear, C. H., Lohmann, G., Poulsen, C. J., Sepulchre, P., Tierney, J. E., Valdes, P. J., Volodin, E. M., Dunkley Jones, T., Hollis, C. J., Huber, M., and Otto-Bliesner, B. L.: DeepMIP: model intercomparison of early Eocene climatic optimum (EECO) large-scale climate features and comparison with proxy data, Clim. Past, 17, 203–227, https://doi.org/10.5194/cp-17-203-2021, 2021.

Lunt, D. J., Foster, G. L., Haywood, A. M., and Stone, E. J.: Late Pliocene Greenland glaciation controlled by a decline in atmospheric CO_2 levels, Nature, 454(7208), 1102–1105, doi:10.1038/nature07223, 2008.

Lunt, D. J., Haywood, A. M., Schmidt, G. A., Salzmann, U., Valdes, P. J., Dowsett, H. J., and Loptson C. A.: On the causes of mid-Pliocene warmth and polar amplification, Earth Planet. Sci. Lett., 321–322(8), 128–138, doi:10.1016/j.epsl.2011.12.042, 2012a.

Lunt, D. J., Dunkley Jones, T., Heinemann, M., Huber, M., LeGrande, A., Winguth, A., Loptson, C., Marotzke, J., Roberts, C. D., Tindall, J., Valdes, P., and Winguth, C.: A model–data comparison for a multi-model ensemble of early Eocene atmosphere–ocean simulations: EoMIP, Clim. Past, 8, 1717–1736, doi:10.5194/cp-8-1717-2012, 2012b.

Murakami, S., Ohgaito, R., Abe-Ouchi, A., Crucifix, M., and Otto-Bliesner, B. L.: Global-scale energy and freshwater balance in glacial climate: A comparison of three PMIP2 LGM simulations, J. Climate, 21, 5008–5033, doi:10.1175/2008jcli2104.1, 2008.

Naish, T., Powell, R., Levy, R., Wilson, G., Scherer, R., Talarico, F., Krissek, L., Niessen, F., Pompilio, M., Wilson, T., Carter, L., DeConto, R., Huybers, P., McKay, R., Pollard, D., Ross, J., Winter, D., Barrett, P., Browne, G., Cody, R., Cowan, E., Crampton, J., Dunbar, G., Dunbar, N., Florindo, F., Gebhardt, C., Graham, I., Hannah, M., Hansaraj, D., Harwood, D., Helling, D., Henrys, S., Hinnov, L., Kuhn, G., Kyle, P., Läufer, A., Maffioli, P., Magens, D., Mandernack, K., McIntosh, W.,

Millan, C., Morin, R., Ohneiser, C., Paulsen, T., Persico, D., Raine, I., Reed, J., Riesselman, C., Sagnotti, L., Schmitt, D., Sjunneskog, C., Strong, P., Taviani, M., Vogel, S., Wilch, T., and Williams, T.: Obliquity-paced Pliocene West Antarctic ice sheet oscillations, Nature, 458(7236), 322–328, doi:10.1038/nature07867, 2009.

Orr, A., Marshall, G. J., Hunt, J. C., Sommeria, J., Wang, C. G., Van Lipzig, N. P., Cresswell, D., and King, J. C.: Characteristics of summer airflow over the Antarctic Peninsula in response to recent strengthening of westerly circumpolar winds, J. Atmos. Sci., 65(4), 1396–1413, doi:10.1175/2007JAS2498.1, 2008.

Pagani, M., Liu, Z., Lariviere, J., and Ravelo, A. C.: High Earth-system climate sensitivity determined from Pliocene carbon dioxide concentrations, Nat. Geosci., 3(1), 27–30, doi:10.1038/NGEO724, 2010.

Parish, T. R., and Bromwich, D. H.: Reexamination of the near-surface airflow over the Antarctic continent and implications on atmospheric circulations at high southern latitudes, Mon. Weather Rev., 135(5), 1961–1973, doi:10.1175/mwr3374.1, 2007.

Patterson, M. O., McKay, R., Naish, T., Escutia, C., Jimenez-Espejo, F. J., Raymo, M. E., Meyers, S. R., Tauxe, L., and Brinkhuis, H.: Orbital forcing of the East Antarctic ice sheet during the Pliocene and Early Pleistocene, Nat. Geosci., 7(11), 841–847, doi:10.1038/ngeo2273, 2014.

Pope, V. D., Gallani, M. L., Rowntree, P. R., and Stratton, R. A.: The impact of new physical parametrizations in the Hadley Centre climate model: HadAM3. Clim. Dynam., 16(2–3), 123–146, 2000.

Raymo, M. E., Lisiecki, L. E., and Nisancioglu, K. H.: Plio-Pleistocene ice volume, Antarctic climate, and the global $\delta^{18}O$ record, Science, 313(5786), 492–495, doi:10.1126/science.1123296, 2006.

Scherer, R. P., DeConto, R. M., Pollard, D., and Alley, R. B.: Windblown Pliocene diatoms and East Antarctic Ice Sheet retreat, Nat. Commun., 7(1), 1–9, doi:10.1038/ncomms12957, 2016.

Schmittner, A., Silva, T. A., Fraedrich, K., Kirk, E., and Lunkeit, F.: Effects of mountains and ice sheets on global ocean circulation, J. Clim., 24(11), 2814–2829

doi:10.1175/2010jcli3982.1, 2011.

Shum, C. K., Kuo, C. Y., and Guo, J. Y.: Role of Antarctic ice mass balance in present-day sea-level change, Polar Sci., 2(2), 149–161, doi:10.1016/j.polar.2008.05.004, 2008.

Tewari, K., Mishra, S. K., Dewan, A., and Ozawa, H.: Effects of the Antarctic elevation on the atmospheric circulation, Theor. Appl. Climatol., 143(3), 1487–1499, doi:10.1007/s00704-020-03456-1, 2021b.

Tewari, K., Mishra, S. K., Dewan, A., Dogra, G., and Ozawa, H.: Influence of the height of Antarctic ice sheet on its climate, Polar Sci., 28, 100642, doi:10.1016/j.polar.2021.100642, 2021a.

Tierney, J. E., Poulsen, C. J., Montañez, I. P., Bhattacharya, T., Feng, R., Ford, H. L., Hönisch, B., Inglis, G. N., Petersen, S. V., Sagoo, N., Tabor, C. R., Thirumalai, K., Zhu, J., Burls, N. J., Foster, G. L., Goddéris, Y., Huber, B. T., Ivany, L. C., Turner, S. K., Lunt, D. J., McElwain, J. C., Mills, B. J. W., Otto-Bliesner, B. L., Ridgwell, A., and Zhang, Y. G.: Past climates inform our future, Science, 370(6517), 1–9, doi:10.1126/science.aay3701, 2020.

Turner, J., Connolley, W. M., Lachlan-Cope, T. A., and Marshall, G. J.: The performance of the Hadley Centre Climate Model (HadCM3) in high southern latitudes, Int. J. Climatol.: A J. Roy. Meteor. Soc., 26(1), 91–112, doi:10.1002/joc.1260, 2006.

Valdes, P. J., Armstrong, E., Badger, M. P. S., Bradshaw, C. D., Bragg, F., Crucifix, M., Davies-Barnard, T., Day, J. J., Farnsworth, A., Gordon, C., Hopcroft, P. O., Kennedy, A. T., Lord, N. S., Lunt, D. J., Marzocchi, A., Parry, L. M., Pope, V., Roberts, W. H. G., Stone, E. J., Tourte, G. J. L., and Williams, J. H. T.: The BRIDGE HadCM3 family of climate models: HadCM3@Bristol v1.0, Geosci. Model Dev., 10, 3715–3743, doi:10.5194/gmd-10-3715-2017, 2017.

Yamane, M., Yokoyama, Y., Abe-Ouchi, A., Obrochta, S., Saito, F., Moriwaki, K., and Matsuzaki, H.: Exposure age and ice-sheet model constraints on Pliocene East Antarctic ice sheet dynamics, Nat. Commun., 6(1), 1–8, doi:10.1038/ncomms8016,

2015.

Yang, S., Ding, Z., Feng, S., Jiang, W., Huang, X., and Guo, L.: A strengthened East Asian Summer Monsoon during Pliocene warmth: Evidence from ‘red clay’ sediments at Pianguan, northern China, J. Asian Earth Sci., 155, 124–133, doi:10.1016/j.jseaes.2017.10.020, 2018.

Zhang, Y.: Projections of 2.0 ºC warming over the globe and China under RCP4.5, Atmos. Oceanic Sci. Lett., 5(6), 514–520, doi:10.1080/16742834.2012.11447047, 2012.

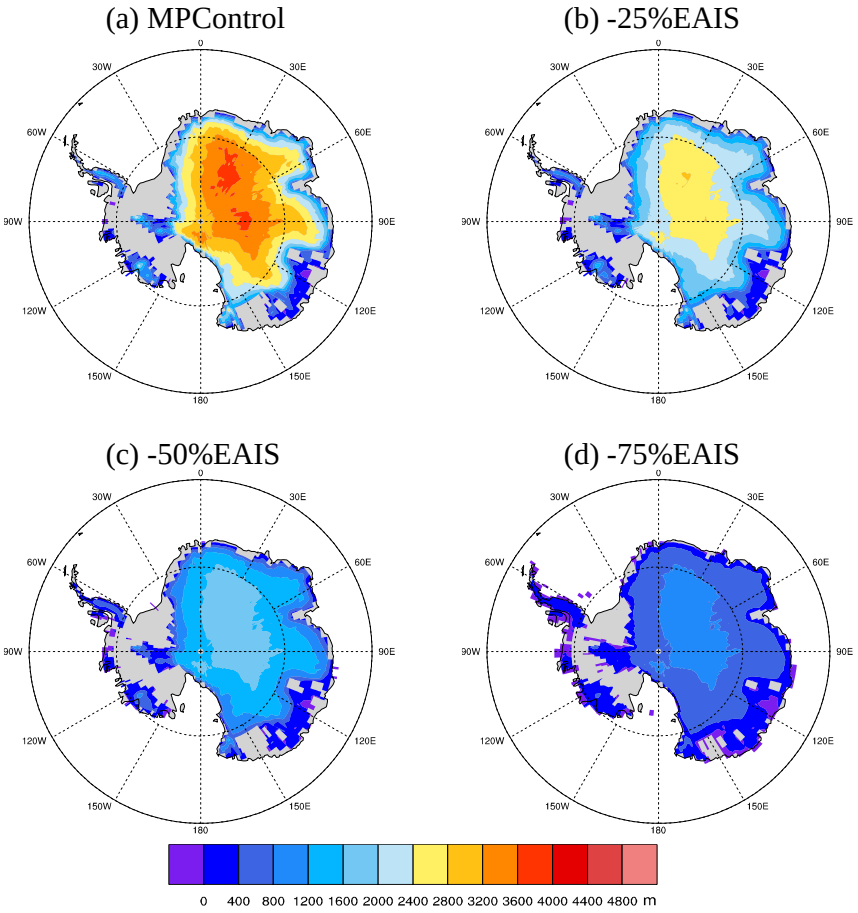

580 Figure 1. The height of the East Antarctic Ice Sheet for the (a) mid-Pliocene control experiment, (b) -25%EAIS sensitivity experiment, (c) -50% EAIS sensitivity experiment, and (d) -75%EAIS sensitivity experiment. It should be noted that, for the -100%EAIS sensitivity experiment, the height of the East Antarctic Ice Sheet has been set to be zero while the surface type is still 'snow'.

585

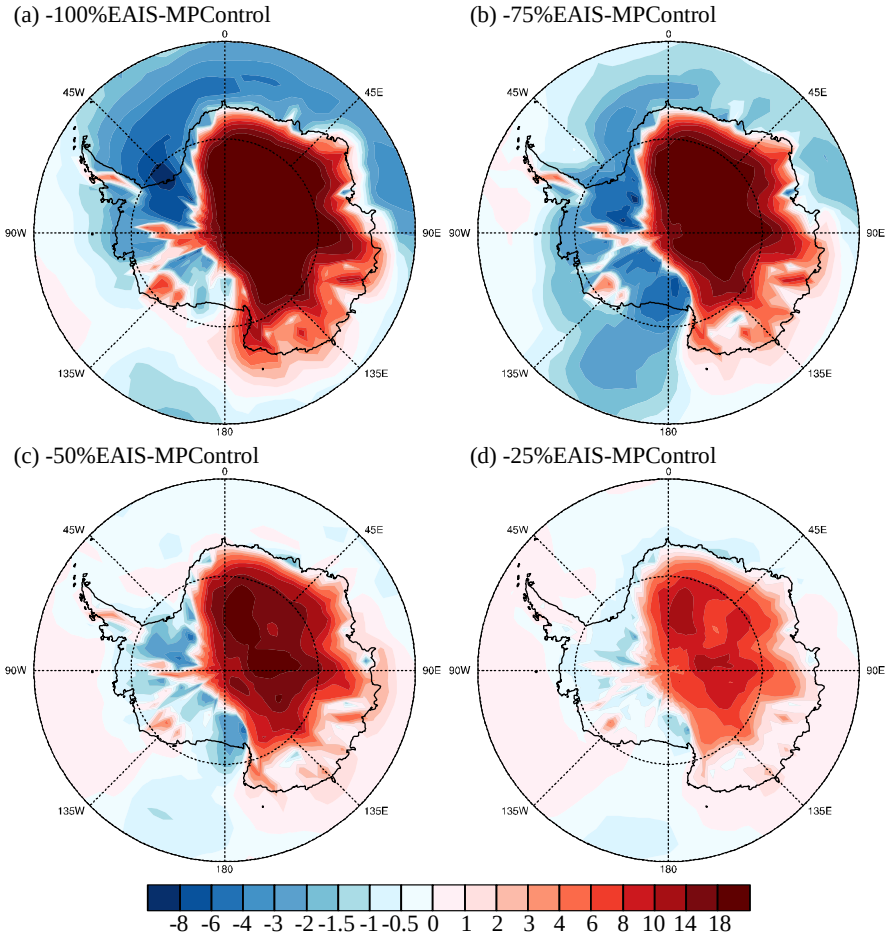

Figure 2. Spatial distribution of the annual mean surface temperature anomalies (units: ℃) over Antarctica between sensitivity experiments and MPControl experiments.

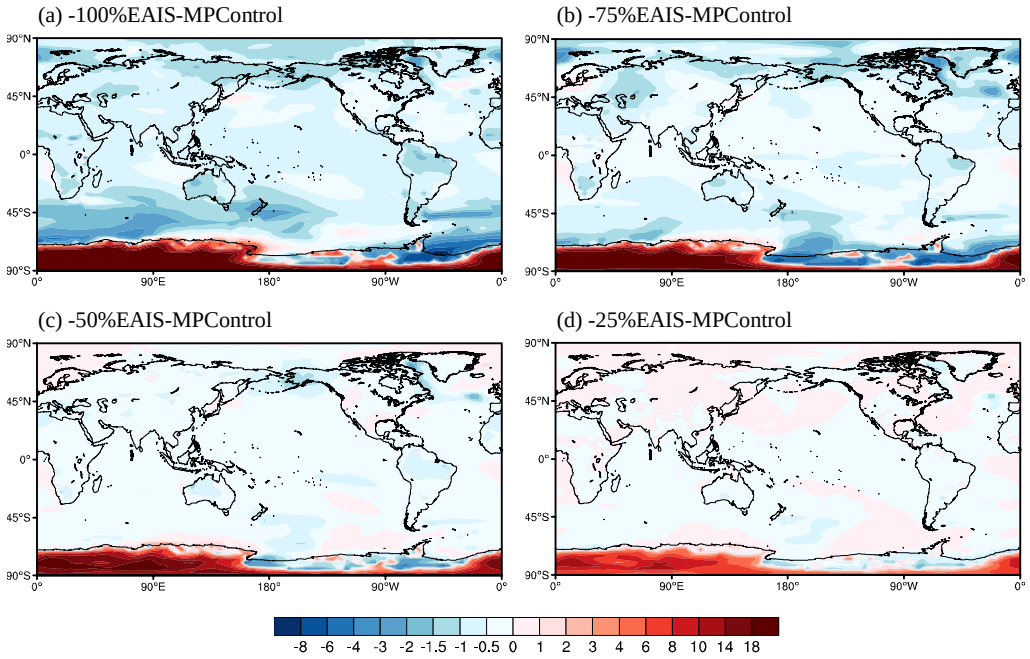

Figure 3. Spatial distribution of the annual mean surface air temperature anomalies (units: ℃) over the globe between sensitivity experiments and MPControl experiments.

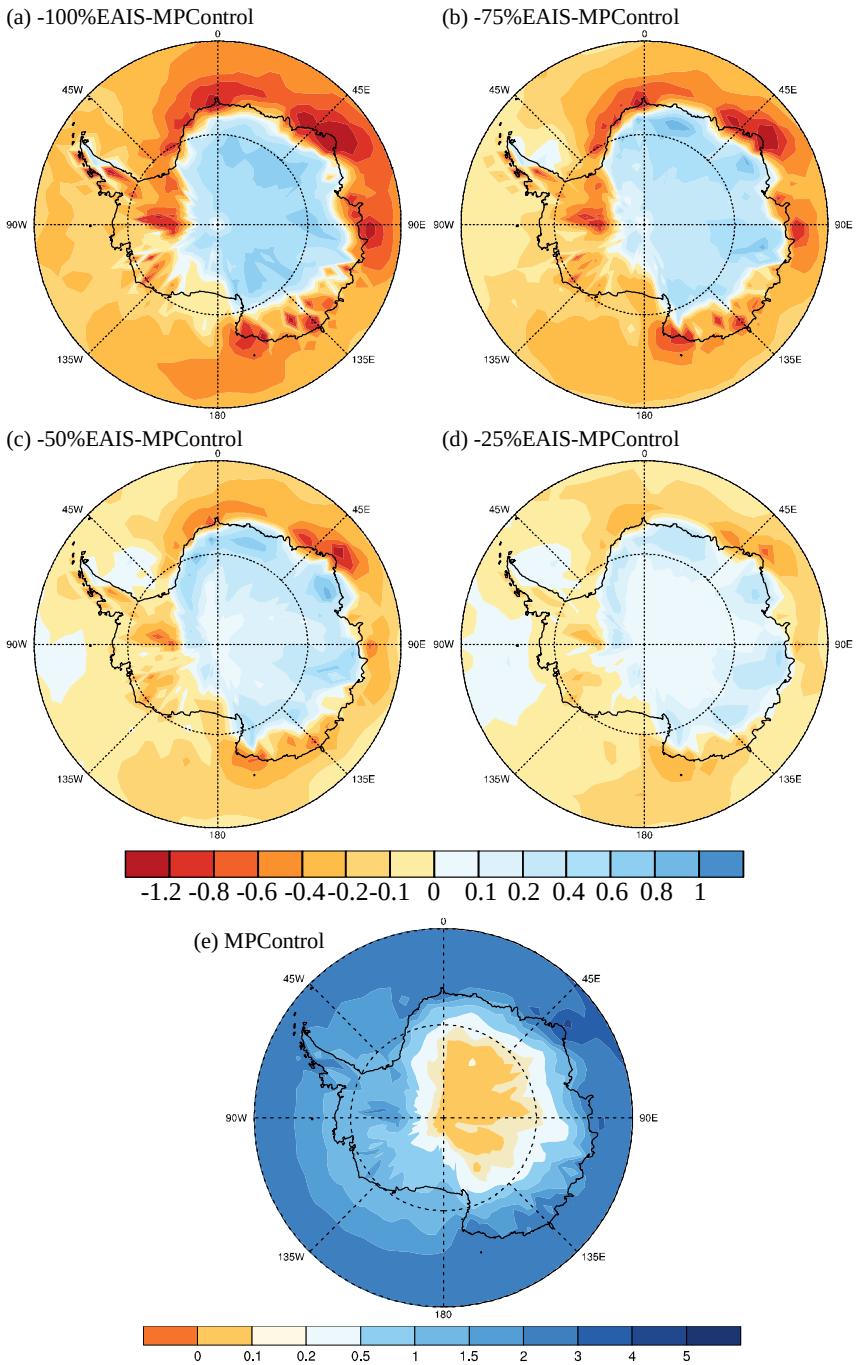

600 Figure 4. Spatial distribution of the annual mean precipitation anomalies (units: mm day^{-1}) over Antarctica between sensitivity experiments and MPControl experiments (a-d), and spatial distribution of the annual mean precipitation over Antarctica for the MPControl experiments (e)

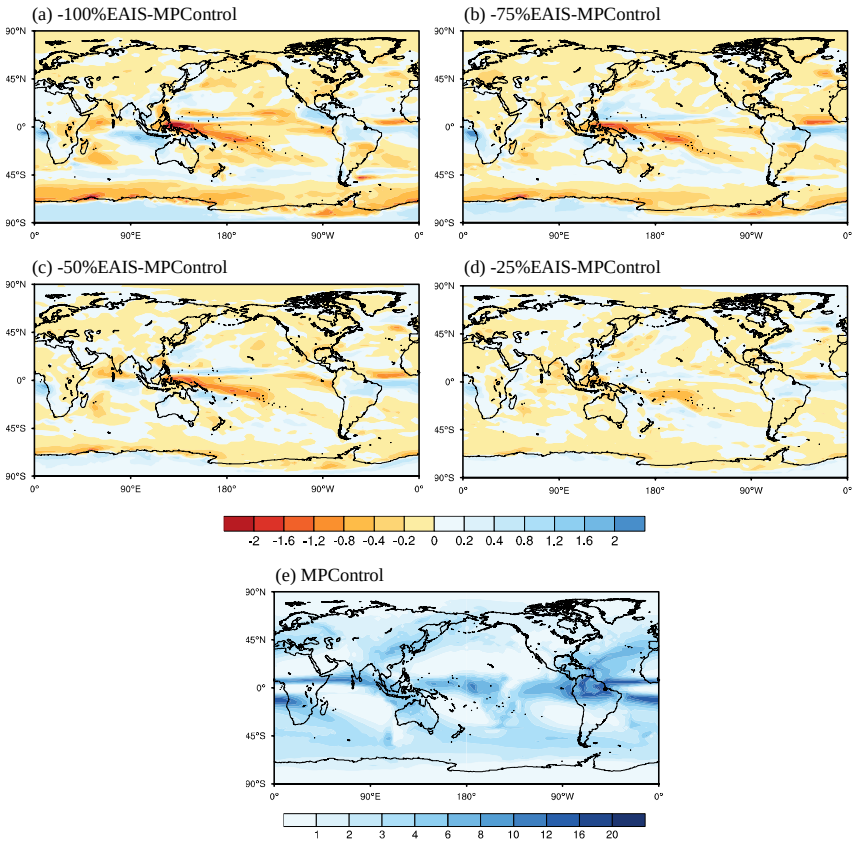

Figure 5. Spatial distribution of the annual mean precipitation anomalies (units: mm day^{-1}) between sensitivity experiments and MPControl experiments (a-d), and spatial distribution of the annual mean precipitation for the MPControl experiments (e).

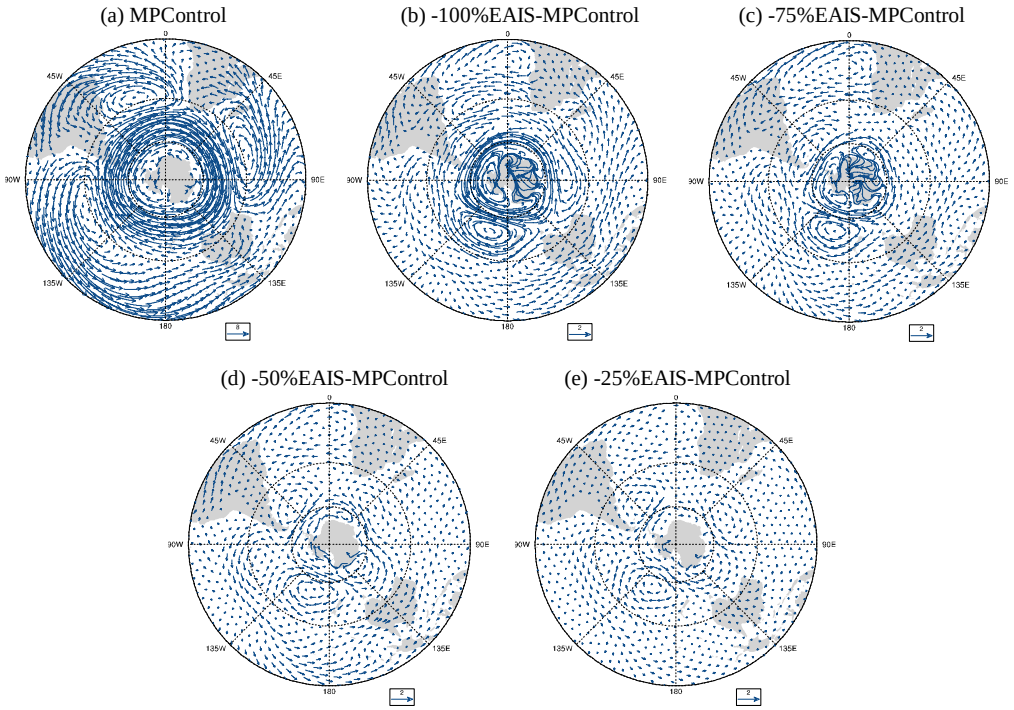

610

Figure 6. Annual mean wind circulation at 850 hPa over the Southern Hemisphere (a; units: m s^{-1}) and its corresponding anomalies in -100%EAIS, -75%EAIS, -50%EAIS, and -25%EAIS, respectively (b-e; units: m s^{-1}).

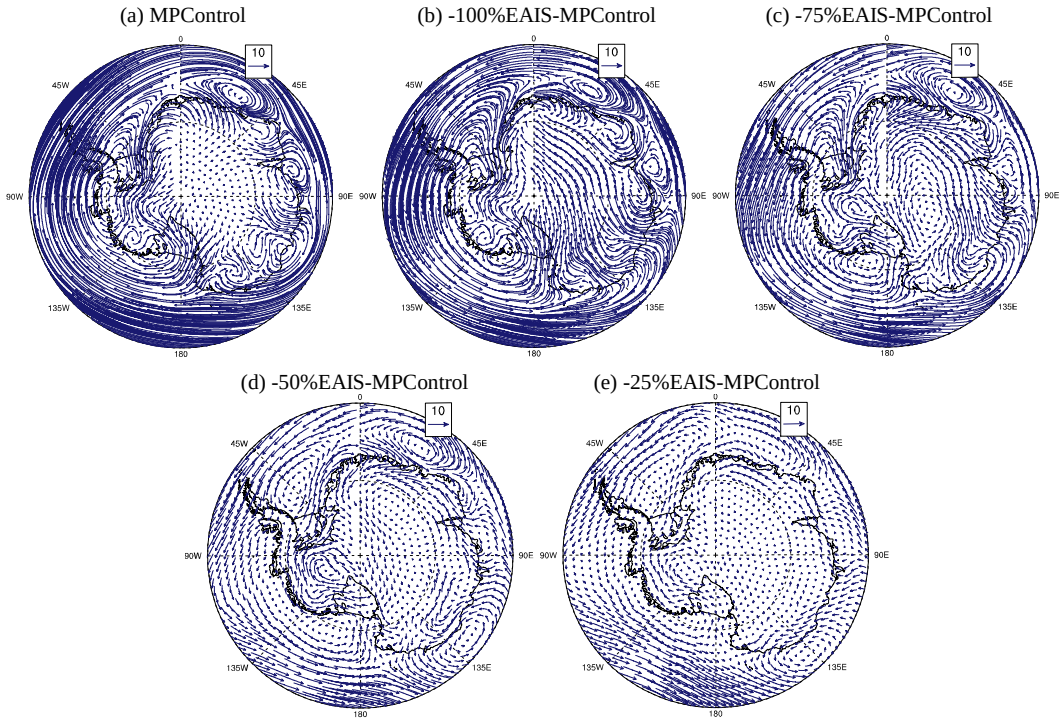

Figure 7. Vertically integrated water vapor flux over Antarctica (arrows, units: kg m^{-1} s^{-1}) for (a) the MPControl, and the anomalies (arrows, units: kg m^{-1} s^{-1}) for (b) the -100%EAIS relative to the MPControl, (c) the -75%EAIS relative to the MPControl, (d) the -50%EAIS relative to the MPControl, and (e) the -25%EAIS relative to the MPControl.

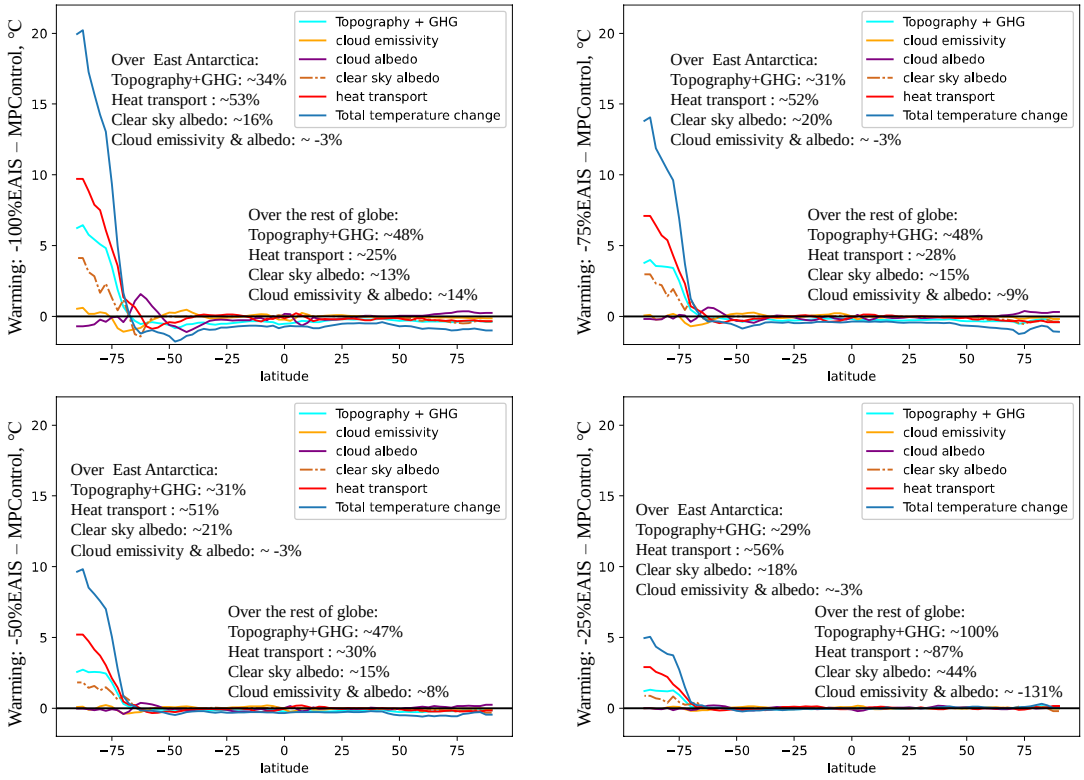

Figure 8. Energy balance analysis between the sensitivity experiments and MPControl. Plot shows the zonal mean warming/cooling at each latitude, from each of the energy balance components. GHG stands for greenhouse gases. The percentage value represents the contribution of each energy balance component to the temperature changes over the East Antarctica and the rest of globe.

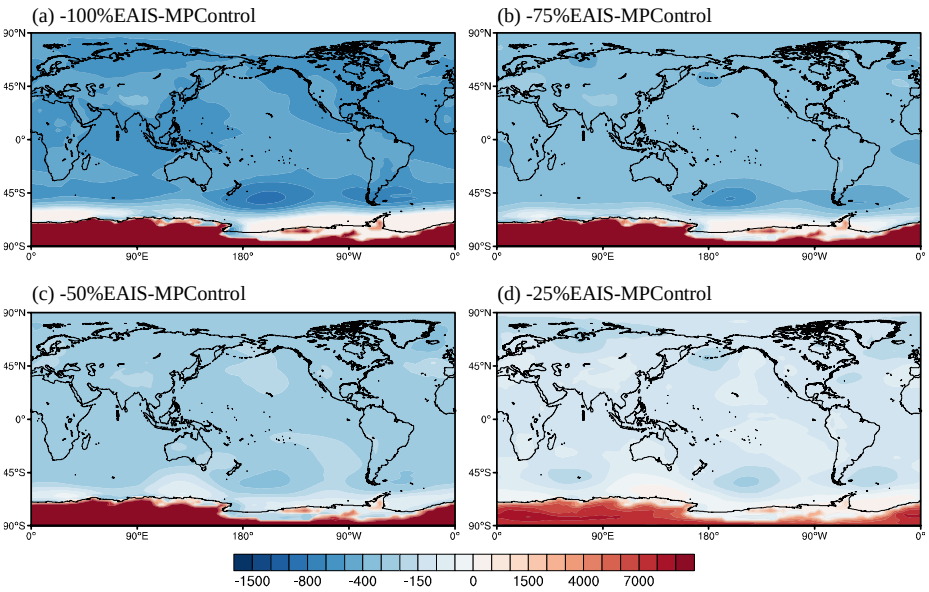

Figure 9. Spatial distribution of the annual mean surface air pressure anomalies (units: Pa) between sensitivity experiments and MPControl experiment.

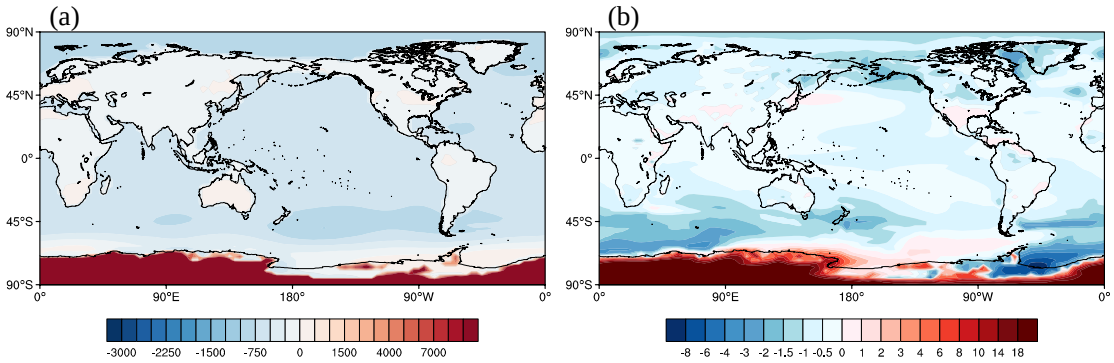

635 Figure 10. Spatial distribution of (a) the annual mean surface air pressure anomalies (units: Pa) and (b) the annual mean surface air temperature (units: ℃) between the new sensitivity experiment and MPControl experiment. The new sensitivity experiment is similar to the -100%EAIS experiment, except artificially raising the sea level by reducing the land level (away from Antarctica) by 60m.

640